Accurate Inertias for Large-Amplitude Motions: Improvements on Prevailing Approximations

Bryan M. Wong, Ryan L. Thom, and Robert W. Field*

Department of Chemistry, Massachusetts Institute of Technology, Cambridge, Massachusetts 02139

Received: December 25, 2005; In Final Form: April 14, 2006

We present a simple yet accurate method for the calculation of effective moments of inertia for large-amplitude low-frequency internal motions in molecules. Our technique makes use of the quantum-mechanical kinetic energy operator developed within the internal coordinate path Hamiltonian formalism, with the imposition of Eckart conditions on the molecular frame to separate the internal motion from overall molecular rotation. Numerical results are presented for several molecules possessing internal large-amplitude motions. These results are compared with those obtained from approximate analytic formulas proposed by Pitzer. We also give detailed examples where the conventional approximations in the current literature are not applicable for describing a single large-amplitude motion. Our straightforward algorithm yields results more accurate than those of Pitzer's method, especially for molecules with asymmetric internal rotors.

I. Introduction

The "separability assumption" of the rigid rotor, harmonic oscillator model is one of the simplest and most extensively used standards for the calculation of spectroscopic quantities in gas-phase molecules. Following this widely adopted assumption, the quantum-mechanical energies are a sum of four separate contributions corresponding to electronic, vibrational, rotational, and translational motions. Since a complete set of molecular energy levels is rarely available, this independent normal-mode approximation is practical and sometimes reasonable. Indeed, the available evidence in standard data tables and the NIST Webbook[1] indicates that this separability approximation permits successful computation of the spectroscopic properties of some stable molecules. However, in many cases, a molecule may contain several low-frequency modes that are not well approximated as small-amplitude harmonic oscillations. The most common example of these floppy modes is an internal rotation about a bond between separate functional groups in a molecule. In addition to internal torsions, other anharmonic motions include bending modes which involve large changes in the angle between two bonds. Uncertainties in how to treat these internal torsions and bending motions can give rise to significant errors in spectroscopic calculations.

When a large-amplitude motion is present, the nuclear Hamiltonian cannot be separated to quadratic order in both the kinetic and potential energy. In addition, one frequently finds that the optimized bond lengths and angles are functions of the large-amplitude coordinate. As a result, the vibrational frequencies of the small-amplitude modes also vary with the large-amplitude coordinate. This raises complex issues about how one should rigorously define the normal coordinates and separate them from the large-amplitude coordinate as well as from the external rotation of the molecule. In many cases, there will be more than one large-amplitude mode, and these will all be coupled together as well as to all of the normal modes. The present paper focuses on the calculation of molecular parameters where only one large-amplitude motion is coupled to the other vibrational modes and to the overall external rotation in molecules. Special emphasis is placed on internal rotations, but the formalism developed in this work is applicable to any large-amplitude motion. A later paper will employ these methods to show how measurement of changes in the dipole moment for excitations along a large-amplitude bending coordinate provides a method to identify particular vibrational levels via the Stark effect.[2]

The conventional approach to computing the effective reduced inertias for internal rotations is through the use of approximate analytical formulas.[3−5] Pitzer and co-workers developed several expressions for reduced moments of inertia which approximately separate the coupling of internal rotation from the overall external rotation of a molecule. As recommended by Pitzer, these protocols are only highly accurate when the moments of inertia for overall rotation are independent of the coordinates of internal rotation[4] (for example, any molecule with rigid symmetrical internal tops such as ethane). However, for molecules with one or more asymmetric internal rotors, the external inertia tensor does depend strongly on the internal rotation coordinate and the Pitzer approximation is less accurate. In certain extreme situations, the rotation of one asymmetric rotor from a trans to a gauche conformation in a massive alkane, for example, can significantly change the principal axes of inertia. Furthermore, Pitzer also stated that if cross terms in the potential energy between internal rotation and vibration are significant, the method of reduced inertias itself may be a crude approximation.[4]

On the other hand, a number of groups have published methods based on Pitzer's formalism.[6−10] However, all of these methods are still based on the approximate treatment of Pitzer, which implicitly neglects both mode−mode coupling and the coupling between internal and external rotation. Here, we show that the conventional Pitzer scheme for estimating the effective inertia can have large differences from inertias obtained by imposing Eckart conditions within an internal coordinate path Hamiltonian formalism. The discrepancies are mostly due to more accurate numerical minimization methods presently avail-

* To whom correspondence should be addressed. E-mail: rwfield@mit.edu. Fax: 001 617 253 7030.

10.1021/jp057504+ CCC: $33.50
Published on Web 05/23/2006

able and are not meant to imply a criticism of Pitzer's earlier work, whose approximate analytical formulas were pioneering at the time they were proposed. In this work, we introduce a rigorous but practical formalism for computing the effective inertia for any type of large-amplitude motion. We present several examples of molecules in which the coupling between the large-amplitude motion and overall rotation is complex. We also provide numerical comparisons with other models on which alternative methods of separating these couplings are based. These examples and comparisons allow assessment of the accuracy of other conventional assumptions routinely used in computing spectroscopic properties.

II. Hamiltonian

The theory of the internal coordinate path Hamiltonian is expressed in terms of a single large-amplitude coordinate s, its conjugate momentum $\hat{p}_s$ ($= -i\hbar\partial/\partial s$), and the coordinates Q_k ($k = 1, 2, ..., 3N - 7$) and momenta $\hat{P}_k$ ($= -i\hbar\partial/\partial Q_k$) of the orthogonal small-amplitude vibrational modes. A detailed method for solving this Hamiltonian using a variational procedure is described by Tew et al.[11] Their formulation is closely related to the reaction path Hamiltonian of Miller, Handy, and Adams[12] with the exception that the internal coordinate path lies on or above the minimum energy path. One of the simplest algorithms to computationally define the minimum energy path is to optimize a saddle point on the potential energy surface and follow the negative gradient of the energy in mass-weighted Cartesian coordinates. However, as Tew et al. have stated, this algorithm is not a numerically sound technique. If the reaction path is not followed with small enough steps, one may not be able to locate the minimum accurately at the end of the path. Furthermore, near the saddle point, the optimized geometries may be inaccurate since the first step away from this starting point is along a vector that does not include any curvature.

The internal coordinate path Hamiltonian used by Tew et al. removes many of these problems by parametrizing a path with a single internal coordinate such as a bond length, a valence bend angle, or in the case of internal rotations, a dihedral angle. The internal coordinate path is defined by keeping a single internal coordinate fixed and minimizing the energy with respect to the other $3N - 7$ degrees of freedom. An internal coordinate is always well-defined at any point on the path and guarantees a continuous variation with no numerical complexity. Since the path is parametrized by an internal coordinate and does not follow the mass-weighted gradient, the internal coordinate path Hamiltonian is invariant under atomic isotope substitution within the molecule. All that remains to define the path is the rotational orientation of the molecular geometries along the internal coordinate parametrization. In what follows, we demonstrate that the effective inertias for large-amplitude motions should only be calculated in a molecule-fixed axis system in which the coupling is minimized between the motion along the path and the rotations of the molecule.

We begin with the quantum-mechanical kinetic energy operator[11]

$$\hat{T} = \frac{1}{2}\sum_{d,e=1}^{4} \mu^{1/4}(\hat{\Pi}_d - \hat{\pi}_d)\mu_{de}\mu^{-1/2}(\hat{\Pi}_e - \hat{\pi}_e)\mu^{1/4} + \frac{1}{2}\sum_{k=1}^{3N-7} \mu^{1/4}\hat{P}_k\mu^{-1/2}\hat{P}_k\mu^{1/4} \quad (1)$$

$\hat{\Pi}$ and $\hat{\pi}$ are four-component operators given by

$$\hat{\Pi} = (\hat{J}_x, \hat{J}_y, \hat{J}_z, \hat{p}_s)$$
$$\hat{\pi} = \sum_{k,l=1}^{3N-7} (B_{kl,x}(s), B_{kl,y}(s), B_{kl,z}(s), B_{kl,s}(s))Q_k\hat{P}_l \quad (2)$$

where $\hat{J}_x$, $\hat{J}_y$, and $\hat{J}_z$ are the components of the total angular momentum operator and $B_{kl,x}$, $B_{kl,y}$, $B_{kl,z}$, and $B_{kl,s}$ are matrices that are functions of the large-amplitude coordinate s. One also requires the following definitions

$$\mu_{de}(s,\mathbf{Q}) = \sum_{a,b=1}^{4} (\mathbf{I}_0 + \mathbf{b})_{da}{}^{-1}\mathbf{I}_{0ab}(\mathbf{I}_0 + \mathbf{b})_{be}{}^{-1}$$
$$\mu(s,\mathbf{Q}) = \det(\mu_{de}) \quad (3)$$

In the following definitions, i and $\alpha\beta\gamma$ denote the ith atom and the xyz Cartesian components, respectively. The augmented symmetric inertia tensor $\mathbf{I}_0$ is

$$\mathbf{I}_0(s) = \begin{pmatrix} I_{0xx}(s) & I_{0xy}(s) & I_{0xz}(s) & I_{0xs}(s) \\ I_{0yx}(s) & I_{0yy}(s) & I_{0yz}(s) & I_{0ys}(s) \\ I_{0zx}(s) & I_{0zy}(s) & I_{0zz}(s) & I_{0zs}(s) \\ I_{0sx}(s) & I_{0sy}(s) & I_{0sz}(s) & I_{0ss}(s) \end{pmatrix} \quad (4)$$

where $I_{0\alpha\beta}$ are the elements of the ordinary 3×3 Cartesian inertia tensor along the path. The other terms $I_{0\alpha s}$ and I_{0ss} are given by

$$I_{0\alpha s}(s) = I_{0s\alpha}(s) = \sum_{i=1}^{N}\sum_{\beta,\gamma=1}^{3} \epsilon_{\alpha\beta\gamma}a_{i\beta}(s)a'_{i\gamma}(s)$$
$$I_{0ss}(s) = \sum_{i=1}^{N}\sum_{\alpha=1}^{3} a'_{i\alpha}(s)a'_{i\alpha}(s) \quad (5)$$

where $\epsilon_{\alpha\beta\gamma}$ is the Levi−Civita antisymmetric tensor. The vectors $\mathbf{a}_i$ ($= m_i^{1/2}\mathbf{r}_i$) are the mass-weighted Cartesian coordinates of the ith atom at a point on the path s with respect to a molecule-fixed axis system and $\mathbf{a}'_i = \mathrm{d}\mathbf{a}_i/\mathrm{d}s$. All that remains is to define $\mathbf{B}$ and $\mathbf{b}$; in the following discussion, we will see it is not necessary to know the explicit forms of these matrices beyond the fact that $\mathbf{B}$ is a function of s, and $\mathbf{b}$ is a 4×4 matrix which is merely linear in Q_k.

$$\mathbf{b}(s) = \sum_{k=1}^{3N-7} Q_k\mathbf{b}_k(s) \quad (6)$$

The exact kinetic energy operator in the full $3N$ coordinates is too complicated to work with directly, and it is necessary to use various approximations to the Hamiltonian which are manageable and physically insightful. The effective moment of inertia matrix depends weakly on the small-amplitude coordinates Q_k.[13] Expanding μ_{de} in the vibrational normal coordinates and retaining the first term depending only on s gives

$$\mu_{de}(s,\mathbf{Q}) = \sum_{a,b=1}^{4} (\mathbf{I}_0 + \mathbf{b})_{da}{}^{-1}\mathbf{I}_{0ab}(\mathbf{I}_0 + \mathbf{b})_{be}{}^{-1} \approx \mathbf{I}_{0de}{}^{-1}(s) \quad (7)$$

Substituting eq 7 into eq 1, and after significant operator algebra (see the Supporting Information), we obtain the approximate kinetic energy operator

$$\hat{T} = \frac{1}{2}\sum_{d,e=1}^{4} \mu_{de}(\hat{\Pi}_d - \hat{\pi}_d)(\hat{\Pi}_e - \hat{\pi}_e) + \frac{1}{2}\sum_{d=1}^{4} (\hat{p}_s\mu_{sd})(\hat{\Pi}_d - \hat{\pi}_d) + \frac{1}{2}\mu^{1/4}(\hat{p}_s\mu_{ss}\mu^{-1/2}(\hat{p}_s\mu^{1/4})) + \frac{1}{2}\sum_{k=1}^{3N-7} \hat{P}_k^{\,2} \quad (8)$$

where the operator $\hat{p}_s$ operates only within the parentheses in eq 8, that is, the next to last term in eq 8 is a scalar pseudopotential term. Since the "vibrational angular momentum" terms, $\hat{\pi}_\alpha$, are linear in the small-amplitude coordinates, Q_k, neglecting their contribution to the kinetic energy gives

$$\hat{T} = \frac{1}{2}\sum_{d,e=1}^{4} \mu_{de}\hat{\Pi}_d\hat{\Pi}_e + \frac{1}{2}\sum_{d=1}^{4} (\hat{p}_s\mu_{sd})\hat{\Pi}_d + \frac{1}{2}\mu^{1/4}(\hat{p}_s\mu_{ss}\mu^{-1/2}(\hat{p}_s\mu^{1/4})) + \frac{1}{2}\sum_{k=1}^{3N-7} \hat{P}_k^{\,2} \quad (9)$$

To remove the terms coupling the total angular momentum with the large-amplitude momentum, one must choose molecule-fixed axes such that $\mu_{\alpha s} = \mu_{s\alpha} = 0$. In other words, if the molecule-fixed axes are chosen such that $I_{0\alpha s} = I_{0s\alpha} = 0$, the effective inverse moment of inertia matrix μ is block diagonal and the kinetic energy operator becomes

$$\hat{T} = \frac{1}{2}\sum_{d,e=1}^{3} \mu_{de}\hat{\Pi}_d\hat{\Pi}_e + \frac{1}{2}\hat{p}_s\mu_{ss}\hat{p}_s + \frac{1}{2}\mu^{1/4}(\hat{p}_s\mu_{ss}\mu^{-1/2}(\hat{p}_s\mu^{1/4})) + \frac{1}{2}\sum_{k=1}^{3N-7} \hat{P}_k^{\,2} \quad (10)$$

Equation 10 implicitly requires numerical enforcement of the Eckart conditions

$$\sum_{i=1}^{N} \mathbf{a}_i(s) \times \mathbf{a}_i'(s) = \mathbf{0} \quad (11)$$

Once the Eckart conditions are satisfied, the effective inverse inertia for the large-amplitude coordinate is given by

$$\mu_{ss}(s) = \left(\sum_{i=1}^{N} \mathbf{a}_i'(s)\cdot\mathbf{a}_i'(s)\right)^{-1} \quad (12)$$

From this expression, one recognizes that $\mu_{ss} = I_{0ss}^{-1}$ is Wilson's[14] G matrix element for the large-amplitude coordinate. The following section describes the computational procedure for calculating this quantity.

III. Eckart Reduced Inertias

We commence by optimizing the molecular geometries using a quantum chemistry computational method while holding a selected internal coordinate s fixed. All conformers of the molecule are translated to a reference frame where the origin is at the center of mass. These molecular geometries are then rotated to a reference frame using the internal axis method (IAM).[15] In the IAM, the axis about which the top executes internal rotation is chosen parallel to one of the coordinate axes. This reference frame is just an intermediate frame which is computationally convenient to compute the Eckart axes later.

The torsional angle dependence of all the mass-weighted Cartesian coordinates of the ith atom in the IAM frame ($a_{i\xi}$, $a_{i\eta}$, $a_{i\zeta}$) is fit to a Fourier series. The corresponding mass-weighted Cartesian coordinates of the ith atom in the Eckart frame are denoted by (a_{ix}, a_{iy}, a_{iz}). The orientation of the Eckart axis system relative to the IAM frame can always be expressed in terms of the Euler angles[14]

$$\begin{bmatrix} a_{ix} \\ a_{iy} \\ a_{iz} \end{bmatrix} = \begin{bmatrix} \lambda_{x\xi} & \lambda_{x\eta} & \lambda_{x\zeta} \\ \lambda_{y\xi} & \lambda_{y\eta} & \lambda_{y\zeta} \\ \lambda_{z\xi} & \lambda_{z\eta} & \lambda_{z\zeta} \end{bmatrix} \begin{bmatrix} a_{i\xi} \\ a_{i\eta} \\ a_{i\zeta} \end{bmatrix} \quad (13)$$

where $\lambda_{\alpha\tau}$ is the direction cosine (which is a function of the Euler angles θ, φ, and χ) of the Eckart α-axis relative to the IAM τ-axis. Using a finite difference approximation for $\mathbf{a}_i'(s)$ gives

$$\mathbf{a}_i'(s_j) \approx \frac{\mathbf{a}_i(s_{j+1}) - \mathbf{a}_i(s_j)}{s_{j+1} - s_j} \quad (14)$$

If the internal coordinate path steps are sufficiently small, the error in estimating $\mathbf{a}_i'(s)$ will also be small. To minimize these numerical errors, we use a Fourier interpolation scheme to estimate the mass-weighted Cartesian coordinates at several points between each optimized geometry in the IAM frame. Substituting the finite difference approximation into eq 11 reduces the Eckart equations to

$$\sum_{i=1}^{N} \mathbf{a}_i(s_j) \times \mathbf{a}_i(s_{j+1}) = \mathbf{0} \quad (15)$$

The three components of this vector equation are

$$\begin{aligned} \sum_{i=1}^{N} [a_{ix}(s_j)a_{iy}(s_{j+1}) - a_{iy}(s_j)a_{ix}(s_{j+1})] &= 0 \\ \sum_{i=1}^{N} [a_{iy}(s_j)a_{iz}(s_{j+1}) - a_{iz}(s_j)a_{iy}(s_{j+1})] &= 0 \\ \sum_{i=1}^{N} [a_{iz}(s_j)a_{ix}(s_{j+1}) - a_{ix}(s_j)a_{iz}(s_{j+1})] &= 0 \end{aligned} \quad (16)$$

The initial geometry in the Eckart frame, defined as the point $s_{j=0}$, is rotated to an orientation which diagonalizes the inertia tensor. To determine the other rotated coordinates at points s_{j+1}, we write eqs 16 in terms of the direction cosines which are functions of the Euler angles θ, φ, and χ. The Cartesian coordinates at points s_{j+1} in the Eckart frame can be expressed in terms of the coordinates at points s_{j+1} in the corresponding IAM frame using eq 13. Therefore

$$\begin{aligned} [x\xi]\lambda_{y\xi} + [x\eta]\lambda_{y\eta} + [x\zeta]\lambda_{y\zeta} - [y\xi]\lambda_{x\xi} - [y\eta]\lambda_{x\eta} - [y\zeta]\lambda_{x\zeta} &= 0 \\ [y\xi]\lambda_{z\xi} + [y\eta]\lambda_{z\eta} + [y\zeta]\lambda_{z\zeta} - [z\xi]\lambda_{y\xi} - [z\eta]\lambda_{y\eta} - [z\zeta]\lambda_{y\zeta} &= 0 \\ [z\xi]\lambda_{x\xi} + [z\eta]\lambda_{x\eta} + [z\zeta]\lambda_{x\zeta} - [x\xi]\lambda_{z\xi} - [x\eta]\lambda_{z\eta} - [x\zeta]\lambda_{z\zeta} &= 0 \end{aligned} \quad (17)$$

where

$$[\alpha\tau] = \sum_{i=1}^{N} a_{i\alpha}(s_j)a_{i\tau}(s_{j+1}) \quad (18)$$

with $\alpha = x$, y, or z, and $\tau = \xi$, η, or ζ. The $\lambda_{\alpha\tau}$ values in eq 17 are the direction cosine matrix elements evaluated at the $j + 1$

TABLE 1: Effective Moments of Inertia Obtained from eqs 12 and 19

	torsional angle (degrees)	U (cm^{-1})	I_{Eckart} [a] (amu Å^2)	I_{Pitzer} [b] (amu Å^2)	I_{Pitzer} [c] (amu Å^2)
		HO−OH			
minimum 1	121.2°	0	0.4373	0.4357	0.3951
		OHC−CHO			
minimum 1	180.0°	0	4.445	4.985	
minimum 2	0.0°	1505	2.818	3.021	
		$H_2CHC-CHCH_2$			
minimum 1	180.0°	0	5.338	6.236	
minimum 2	37.8°	936.8	3.460	4.589	
		FH_2C-CH_2F			
minimum 1	69.0°	0	9.390	8.749	
minimum 2	180.0°	74.83	8.490	8.910	
		ClH_2C-CH_2F			
minimum 1	180.0°	0	11.05	11.55	18.37
minimum 2	65.9°	164.9	11.34	11.59	25.28
		ClH_2C-CH_2Cl			
minimum 1	180.0°	0	15.76	16.37	17.56
minimum 2	68.2°	531.7	15.15	17.84	207.8

[a] Using eq 12. [b] Using eq 19. [c] Literature values from ref 10.

point. The geometry $a_{i\alpha}(s_j)$ in the Eckart frame and the geometry $a_{i\tau}(s_{j+1})$ in the IAM frame are known quantities, so eq 17 is a set of three simultaneous transcendental equations involving only the three Euler angles. We solve this nonlinear system of equations using the Powell dogleg method.[16] This system of equations is highly nonlinear and can require several function evaluations to reach convergence. In our computer program available via the Internet,[17] we have implemented analytical Jacobians in the dogleg method to maximize computational efficiency. This system of transcendental equations is solved iteratively with initial guesses of the Euler angles at point s_{j+1} taken from the known Euler angles at point s_j. After this procedure is carried out for all the geometries ($a_{i\xi}$, $a_{i\eta}$, $a_{i\zeta}$), a finite difference approximation can be used to obtain (a'_{ix}, a'_{iy}, a'_{iz}) in the Eckart frame and one has all the information needed to calculate the effective inertia in eq 12.

IV. Pitzer Reduced Inertias

The method of calculating the effective moment of inertia with Pitzer's formulas is well-known,[3−5,8,10] and we only briefly review the method in this section. Pitzer's expression for the reduced moment of inertia for a single internal rotation is given by

$$I = A - \sum_i \left[\frac{(\alpha^{iy} U)^2}{M} + \frac{(\beta^i)^2}{I_i} \right] \tag{19}$$

where

$$\beta^i = \alpha^{iz} A - \alpha^{ix} B - \alpha^{iy} C + U(\alpha^{i-1,y} r^{i+1} - \alpha^{i+1,y} r^{i-1}) \tag{20}$$

The superscripts $i-1$ and $i+1$ are cyclic indices such that if $i = 1$, $i-1 = 3$, and if $i = 3$, $i+1 = 1$. The array

$$\begin{bmatrix} \alpha^{1x} & \alpha^{2x} & \alpha^{3x} \\ \alpha^{1y} & \alpha^{2y} & \alpha^{3y} \\ \alpha^{1z} & \alpha^{2z} & \alpha^{3z} \end{bmatrix} \tag{21}$$

is the direction cosines between the axes of the rotating top (x, y, z) and the axes of the whole molecule (1, 2, 3). The internal rotation axis is taken as the z-axis of the top, and the x-axis passes through the top's center of mass. The axes of the whole molecule are those which pass through the center of mass and diagonalize the inertia tensor. All of Pitzer's expressions are based on the kinetic energy expression of Kassel[18] and Crawford,[19] which uses a principal axis method (PAM)[15] for molecular-fixed axes. It should be noted that these and the following expressions give the same results whether one includes or does not include atoms on the axis of rotation as part of the top. The following quantities are defined only with respect to the coordinate system of the top, which is composed of the ith atom with mass m_i

$$\begin{aligned} A &= \sum_i m_i (x_i^2 + y_i^2) \\ B &= \sum_i m_i x_i z_i \\ C &= \sum_i m_i y_i z_i \\ U &= \sum_i m_i x_i \end{aligned} \tag{22}$$

Finally, the components of the vector (r^1, r^2, r^3) in eq 20 point from the center of gravity of the whole molecule in the PAM reference frame to the origin of coordinates of the top.

V. Examples and Applications

In Table 1, we compare the results of eq 12 against eq 19 for several molecules that have a single unsymmetrical torsion. Table 1 also gives the parameters characterizing the local minima along the torsional coordinate for each molecule: U is the torsional potential energy of a local minimum relative to the globally lowest minimum, I_{Eckart} is the effective inertia calculated from eq 12, and I_{Pitzer} is the effective inertia calculated from eq 19. All ab initio electronic structure calculations for these molecules were carried out with the Gaussian 03 package[20] using the second-order Møller−Plesset perturbation level of theory for all electrons (MP2(full)). The standard 6-31G(d) basis set with the MP2(full) level of theory used in the present work is the same methodology employed in geometry optimizations in Pople's G3 composite procedures.[21] The point of the calculations presented is to provide reasonable and consistent geometries to test the accuracy of other conventional assumptions used in computing effective inertias. The purpose is not to resolve the many open questions regarding how best to calculate ab initio torsional potentials on the specific molecules presented as illustrative examples. For each molecule, the torsional potential was calculated by constraining a dihedral angle and optimizing all other internal coordinates to minimize the total energy.

Of the six molecules listed in Table 1, hydrogen peroxide, 1,2-dichloroethane, and 1-fluoro-2-chloroethane were previously analyzed by Chuang and Truhlar.[10] The last column of Table 1 lists the available literature values from Chuang and Truhlar, who also used the same Pitzer approximation described in section IV of the present work. We draw attention to the large deviation of their results from our calculations, especially for the case of 1,2-dichloroethane, ClH_2C-CH_2Cl. Extensive theoretical[7,22−24] and a few experimental[25,26] studies have already been carried out on this asymmetric torsional motion. One of the first studies on 1,2-dichloroethane in the current literature is the finite-difference-boundary-value treatment by Chung-

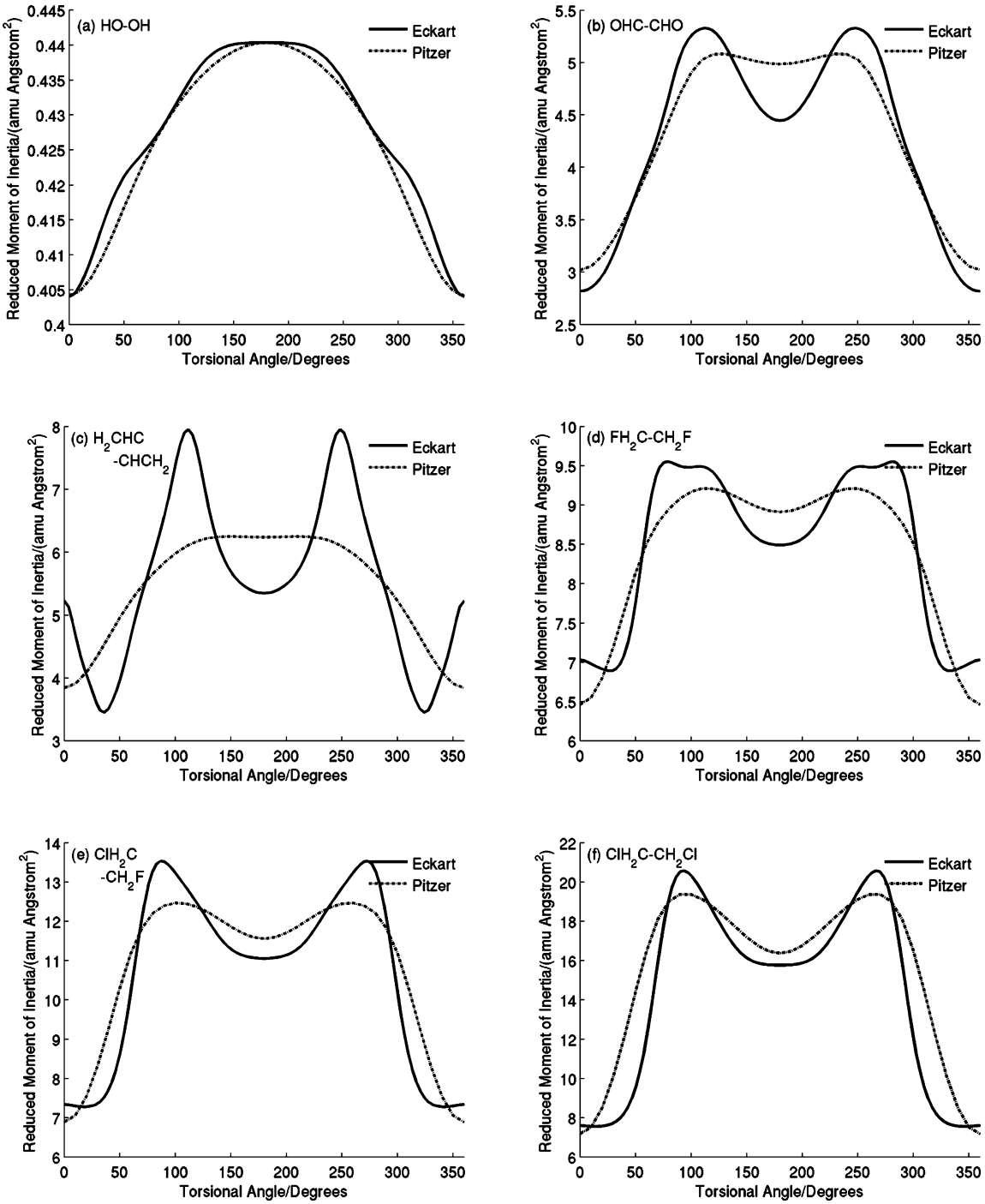

Figure 1. (a−f) Eckart effective inertias (eq 12) for six molecules displaying internal rotation compared with those calculated from Pitzer's formulas (eq 19).

Phillips.[22] Her analysis includes an ab initio calculation of the relaxed geometries and torsional potential performed at the HF/6-31G* level of theory. Using the HF/6-31G* adiabatic potential energy curve, Chung-Phillips calculated one trans minimum and two equivalent gauche minima with I_{Pitzer} values of 16.46 and 17.93 amu Å^2, respectively. Although the Hartree−Fock method used in her work is not quantitatively accurate, her two values of I_{Pitzer} are still in extraordinary agreement with our calculations in Table 1. More recently, Ayala and Schlegel have revisited the calculation of I_{Pitzer} for 1,2-dichloroethane and found in section III of their work that the reduced moment of inertia increases only by a factor of 2 (in contrast to Chuang and Truhlar's factor of 12) as the twist angle is varied.[7] One of the latest studies on 1,2-dichloroethane torsional motion is from the work of Hnizdo and co-workers, who have used the Pitzer formalism to estimate entropies of internal rotation via Monte Carlo simulations.[24] In Figure 2 of their work, they have plotted the variation of $I_{\text{Pitzer}}^{1/2}$ as a function of the torsional angle, and they obtain results which are in excellent agreement with Figure 1f of the present work. The good consistency of our results with respect to these three literature values supports our tabulated values, and our method of calculating I_{Pitzer} appears to be well-justified.

Figure 1 compares the Eckart and Pitzer effective inertias for the six molecules listed in Table 1. For each figure, both the Eckart and Pitzer inertias were calculated using the same molecular geometries on a regular grid of 10° increments for the torsional angle. An interesting feature of these figures is

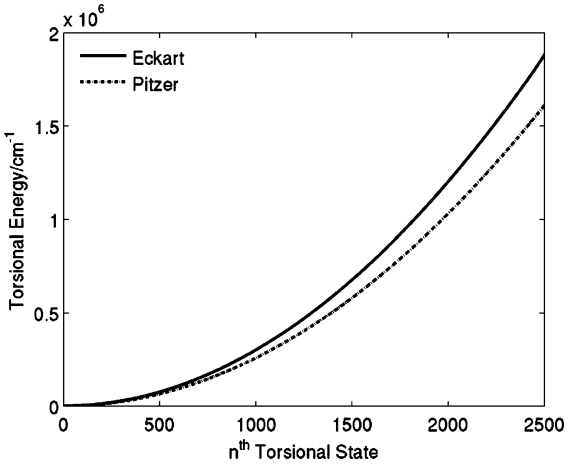

Figure 2. Lowest 2500 eigenvalues for the torsional motion of 1,2-dichloroethane. The eigenvalues obtained from the instantaneous Eckart inertias are considerably larger than those obtained from a constant-valued Pitzer inertia at the trans geometry.

that both methods yield similar results for H_2O_2, but the differences between the two methods become more significant as the rotating top becomes more asymmetric. Among these calculations, we see considerable quantitative and qualitative discrepancies between the two methods for 1,3-butadiene. The torsional potential energy surface of 1,3-butadiene has a local minimum near 40° corresponding to a gauche configuration. At this value of the torsional angle, the Eckart effective inertia also has a minimum but this feature is absent in the Pitzer calculations. For the asymmetric torsions studied, it is apparent the Eckart effective inertias show more structure and variation as a function of torsional angle than the corresponding Pitzer inertias.

To demonstrate the effects of using the Eckart and Pitzer formalisms on dynamical properties, we calculate a converged set of eigenvalues and eigenvectors for 1,2-dichloroethane utilizing the one-dimensional kinetic energy operator given by the first three terms of eq 10. Figure 2 compares the lowest 2500 torsional energies evaluated (1) using the instantaneous Eckart inertias displayed in Figure 1f and (2) using only the constant value of the Pitzer inertia at the global trans minimum. Both methods give eigenvalues close to each other for torsional quanta less than 50, but the eigenvalues obtained from the instantaneous Eckart calculations are generally much larger than the results derived from the constant Pitzer inertia. The differences between the two methods are even more pronounced when the number of torsional quanta becomes greater than 100, and after 2500 quanta of the torsion is reached, the Eckart eigenvalues are larger than the Pitzer eigenvalues by more than 272 000 cm^{-1}. This discrepancy can be simply understood realizing that the allowed eigenvalues for free rotation in one dimension are $E_m = m^2\hbar^2/2I$ with $m = 0, \pm1, \pm2, ...$ For 1,2-dichloroethane at our simple MP2 level of theory, this free rotation limit is only reached when the number of torsional quanta exceeds 90 and the eigenvalues become doubly degenerate as shown in Figure 3a. Below the free rotation limit, the torsional wave functions have distinct, nondegenerate energies corresponding to alternating symmetric (red-colored) and antisymmetric (green-colored) torsional states.

Figure 3b shows the 150 lowest torsionally averaged Eckart inertias, $\langle I_{Eckart}\rangle$, of 1,2-dichloroethane obtained by evaluating the instantaneous Eckart inertias in Figure 1f averaged over each of the torsional wave functions. The averaged Eckart inertias are also color-coded to match their symmetric (red)/antisymmetric (green) energy levels in Figure 3a. The dotted horizontal line is the numerical value for the Pitzer effective inertia evaluated at the trans global minimum. For $n < 5$, $\langle I_{Eckart}\rangle$ does not vary appreciably from 15.76 amu Å^2 since the torsional wave function is localized in the trans global minimum. For $5 < n < 90$, $\langle I_{Eckart}\rangle$ varies rapidly since the torsional wave function alternates between the two gauche local minima and the single trans minimum. As discussed previously, the torsion is nearly a free rotation for $n > 90$, and $\langle I_{Eckart}\rangle$ is approximately constant with a limiting value of approximately 15.1 amu Å^2. Since the free rotation energy, E_m, is proportional to I^{-1}, basing the torsional energies on the larger Pitzer inertia would significantly underestimate the Eckart eigenvalues above the free rotation limit (cf. Figure 2).

As a final application, we calculate the effective inertia for the large-amplitude motion describing the isomerization of acetylene to vinylidene. Since we are primarily interested in the local bender limit of this 1,2-hydrogen rearrangement process, the most intuitive choice for the large-amplitude parameter s is the internal HCC bend angle in acetylene. While CC−HH diatom−diatom coordinates are much better suited for describing vinylidene and H-atom orbiting states,[27−28] they are more awkward to use at low energies below the vinylidene isomerization barrier.[29−31] For this reason, we obtained our internal coordinate path by constraining the HCC angle at 5° increments while optimizing all other internal coordinates to minimize the total energy. The electronic structure calculations for the relaxed molecular geometries of acetylene were carried

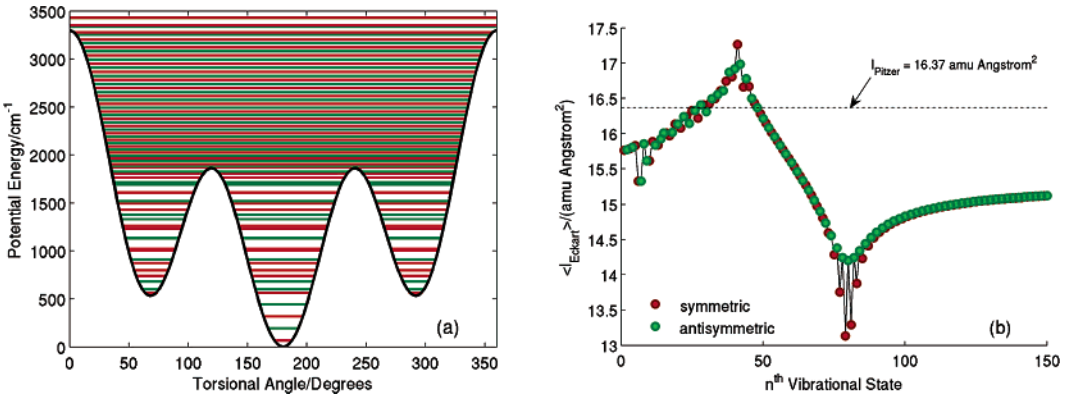

Figure 3. (a) Relaxed torsional potential and energies for 1,2-dichloroethane obtained at the MP2(full)/6-31G(d) level of theory. Each of the torsional eigenvalues is associated with symmetric (red-colored) and antisymmetric (green-colored) torsional states. (b) Torsionally averaged Eckart inertias, $\langle I_{Eckart}\rangle$, for the lowest 150 torsional states of 1,2-dichloroethane. The broken line indicates the numerical value of $I_{Pitzer} = 16.37$ amu Å^2 calculated at the trans global minimum.

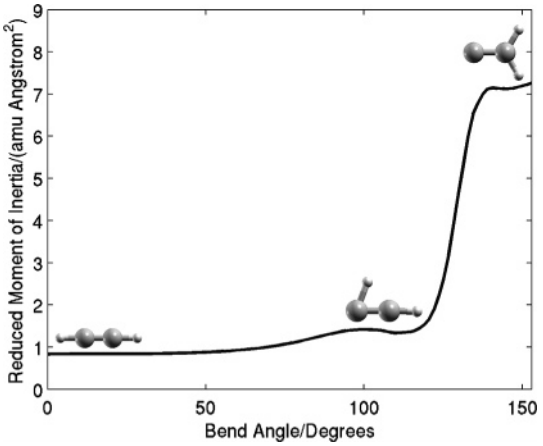

Figure 4. Reduced moment of inertia calculated by our algorithm for the HCC bending motion of acetylene. The effective inertia increases rapidly near 110° when the right-most hydrogen moves in concert with the left-most hydrogen to form vinylidene.

out using the coupled cluster with single and double substitutions level of theory for all electrons (CCSD(full)). The basis set used at this level of theory was Dunning's augmented correlation consistent triple-ζ basis, aug-cc-pvtz.[32]

Figure 4 shows the effective inertia as a function of the bend angle up to a final value of 153°, which corresponds to the equilibrium geometry of vinylidene. The method of Pitzer cannot be applied to this type of large-amplitude motion, but the effective inertia can still be calculated easily by solving eq 12 as described in section III. As shown in Figure 4, the isomerization from acetylene to vinylidene involves one hydrogen migrating a large distance off the C−C bond axis while the other hydrogen remains relatively stationary. The transition state structure for the isomerization process emerges when the active hydrogen makes an angle of approximately 110° as measured from the equilibrium linear geometry. Once the HCC bend angle is increased past the transition state structure, large variations in geometries occur as the right-most hydrogen moves in concert with the left-most hydrogen and the C−C triple bond lengthens to a double bond. Since the Eckart inertia is proportional to $\mathbf{a}'_i(s)\cdot\mathbf{a}'_i(s)$ (cf. eq 12), and the geometry changes rapidly past the transition state, the effective inertia is significantly larger for HCC bend angles greater than 110°. In a later paper, this method has been used in conjunction with an effective Hamiltonian model to describe the Stark effect as a diagnostic tool for recognizing and assigning local-bender excited vibrational states.[2]

VI. Conclusion

We have presented a method by which accurate inertias for internal rotations and other large-amplitude motions may be calculated by rigorously separating this motion from the external rotation. It was shown that the conventional Pitzer scheme for estimating the effective inertia can result in large differences from the Eckart method, which minimizes the couplings of torsions to rotations. This is apparent if one remembers that the Pitzer method is inherently based on a coordinate system used from PAM. If the rotating top has an axis of symmetry, the principal axes of the molecule do not change significantly as the torsional angle is varied. However, if both the rotating top and the frame of the molecule are heavy and asymmetric, the cross terms which represent the interactions between the two kinds of rotation (cf. eq 9) are much larger in PAM/Pitzer's method than in the Eckart frame. To correct this inadequacy, it is necessary to go beyond approximate analytical formulas to pursue numerical methods of minimizing these couplings.

We also show that the Eckart method is general and applies to other large-amplitude motions such as large variations in angle bends. In a one-dimensional description of the acetylene/vinylidene isomerization, the procedure is essential since it minimizes several of the coupling terms between the large-amplitude bend and the overall rotation. This is particularly important since the relaxed geometries describing the 1,2-hydrogen rearrangement do not change uniformly along the isomerization path. A user-friendly code for computing the Eckart inertia as a function of the torsional angle is available.[17] These computer programs automatically solve the nonlinear set of equations in eq 17 and output the reduced inertias as a function of the torsional angle. All of the examples presented in Table 1 are also available as sample inputs for these codes. We recommend the Eckart method described in section III as an alternative to the conventional Pitzer method when asymmetric tops are present.

Acknowledgment. All ab initio calculations and algorithm developments were performed on a custom-built server at the Sidney-Pacific Residence at the Massachusetts Institute of Technology, which comprises two processors (2 × 2.8 GHz Intel Xeon), with a total of 4 Gb of RAM. This research was supported by the Office of Basic Energy Sciences, Offices of Energy Research, U.S. Department of Energy under Grant No. DE-FG0287ER13671.

Supporting Information Available: Several intermediate steps in the derivation of eq 8. This material is available free of charge via the Internet at http://pubs.acs.org.

References and Notes

(1) http://webbook.nist.gov/chemistry (accessed December 25, 2005).
(2) Wong, B. M.; Steeves, A. H.; Field, R. W. *J. Phys. Chem. A*, submitted for publication, March 28, 2006.
(3) Pitzer, K. S.; Gwinn, W. D. *J. Chem. Phys.* **1942**, *10*, 428−440.
(4) Pitzer, K. S. *J. Chem. Phys.* **1946**, *14*, 239−243.
(5) Pitzer, K. S.; Kilpatrick, J. E. *J. Chem. Phys.* **1949**, *17*, 1064−1075.
(6) McClurg, R. B.; Flagan, R. C.; Goddard, W. A., III. *J. Chem. Phys.* **1997**, *106*, 6675−6680.
(7) Ayala, P. Y.; Schlegel, H. B. *J. Chem. Phys.* **1998**, *108*, 2314−2325.
(8) East, A. L. L.; Radom, L. *J. Chem. Phys.* **1997**, *106*, 6655−6674.
(9) Truhlar, D. G. *J. Comput. Chem.* **1991**, *12*, 266−270.
(10) Chuang, Y.; Truhlar, D. G. *J. Chem. Phys.* **2000**, *112*, 1221−1228.
(11) Tew, D. P.; Handy, N. C.; Carter, S.; Irle, S.; Bowman, J. *Mol. Phys.* **2003**, *101*, 3513−3525.
(12) Miller, W. H.; Handy, N. C.; Adams, J. E. *J. Chem. Phys.* **1980**, *72*, 99−112.
(13) Rao, K. N.; Mathews, C. W. *Molecular Spectroscopy: Modern Research*; Academic Press: New York, 1972.
(14) Wilson, E. B., Jr.; Decius, J. C.; Cross, P. C. *Molecular Vibrations: The Theory of Infrared and Raman Vibrational Spectra*; Dover Publications: New York, 1955.
(15) Lin, C. C.; Swalen, J. D. *Rev. Mod. Phys.* **1959**, *31*, 841−892.
(16) Rabinowitz, P. *Numerical Methods for Nonlinear Algebraic Equations*; Gordon and Breach Science Publishers: New York, 1970.
(17) http://rwf.lms.mit.edu/group/lib.html.
(18) Kassel, L. S. *J. Chem. Phys.* **1936**, *4*, 276−282.
(19) Crawford, B. L., Jr. *J. Chem. Phys.* **1940**, *8*, 273−281.
(20) Frisch, M. J.; Trucks, G. W.; Schlegel, H. B.; Scuseria, G. E.; Robb, M. A.; Cheeseman, J. R.; Montgomery, J. A., Jr.; Vreven, T.; Kudin, K. N.; Burant, J. C.; Millam, J. M.; Iyengar, S. S.; Tomasi, J.; Barone, V.; Mennucci, B.; Cossi, M.; Scalmani, G.; Rega, N.; Petersson, G. A.; Nakatsuji, H.; Hada, M.; Ehara, M.; Toyota, K.; Fukuda, R.; Hasegawa, J.; Ishida, M.; Nakajima, T.; Honda, Y.; Kitao, O.; Nakai, H.; Klene, M.; Li, X.; Knox, J. E.; Hratchian, H. P.; Cross, J. B.; Bakken, V.; Adamo, C.; Jaramillo, J.; Gomperts, R.; Stratmann, R. E.; Yazyev, O.; Austin, A. J.; Cammi, R.; Pomelli, C.; Ochterski, J. W.; Ayala, P. Y.; Morokuma, K.; Voth, G. A.; Salvador, P.; Dannenberg, J. J.; Zakrzewski, V. G.; Dapprich,

S.; Daniels, A. D.; Strain, M. C.; Farkas, O.; Malick, D. K.; Rabuck, A. D.; Raghavachari, K.; Foresman, J. B.; Ortiz, J. V.; Cui, Q.; Baboul, A. G.; Clifford, S.; Cioslowski, J.; Stefanov, B. B.; Liu, G.; Liashenko, A.; Piskorz, P.; Komaromi, I.; Martin, R. L.; Fox, D. J.; Keith, T.; Al-Laham, M. A.; Peng, C. Y.; Nanayakkara, A.; Challacombe, M.; Gill, P. M. W.; Johnson, B.; Chen, W.; Wong, M. W.; Gonzalez, C.; Pople, J. A. *Gaussian 03*, revision B.05; Gaussian, Inc.: Wallingford, CT, 2004.

(21) Curtiss, L. A.; Raghavachari, K.; Redfern, P. C.; Rassolov, V.; Pople, J. A. *J. Chem. Phys.* **1998**, *109*, 7764−7776.

(22) Chung-Phillips, A. *J. Comput. Chem.* **1992**, *13*, 874−882.

(23) El Youssoufi, Y.; Herman, M.; Liévin, J. *Mol. Phys.* **1998**, *94*, 461−472.

(24) Hnizdo, V.; Fedorowicz, A.; Singh, H.; Demchuk, E. *J. Comput. Chem.* **2003**, *24*, 1172−1183.

(25) El Youssoufi, Y.; Georges, R.; Liévin, J.; Herman, M. *J. Mol. Spectrosc.* **1997**, *186*, 239−245.

(26) El Youssoufi, Y.; Liévin, J.; Vander Auwera, J.; Herman, M. *Mol. Phys.* **1998**, *94*, 473−484.

(27) Zou, S.; Bowman, J. M. *Chem. Phys. Lett.* **2003**, *368*, 421−424.

(28) Zou, S.; Bowman, J. M.; Brown, A. *J. Chem. Phys.* **2003**, *118*, 10012−10023.

(29) Liu, L.; Muckerman, J. T. *J. Chem. Phys.* **1997**, *107*, 3402−3416.

(30) Xu, D.; Li, G.; Xie, D.; Guo, H. *Chem. Phys. Lett.* **2002**, *365*, 480−486.

(31) Xu, D.; Chen, R.; Guo, H. *J. Chem. Phys.* **2003**, *118*, 7273−7282.

(32) Kendall, R. A.; Dunning, T. H., Jr.; Harrison, R. J. *J. Chem. Phys.* **1992**, *96*, 6796−6806.